

# Measuring attosecond pulses generated from polarization gating

Z. X. Zhao, Zenghu Chang, X. M. Tong and C. D. Lin

Physics Department, Kansas State University, Manhattan, KS, 66506, USA

## ABSTRACT

Angle-resolved photoelectron spectra of argon atoms by XUV attosecond pulses in the presence of a circularly polarized laser field are calculated to examine their dependence on the duration and the chirp of the attosecond pulses. From the calculated electron spectra, we show how to retrieve the duration and the chirp of the attosecond pulse using genetic algorithm. The method is expected to be used for characterizing the attosecond pulses which are produced by polarization gating of few-cycle left- and right-circularly polarized infrared laser pulses.

**Keywords:** Attosecond pulses, ultrafast measurements, photionization, polarization gating

## 1. INTRODUCTION

Single attosecond extreme ultraviolet (XUV) or soft x-ray pulses can be generated by high-order harmonic generation with few-cycle femtosecond infrared (IR) laser pulses.<sup>1</sup> Their short wavelength and weak intensity means that conventional autocorrelation method cannot be used to determine their pulse durations directly. So far, pulse duration has been determined with laser-assisted photoionization where photoelectron spectra by XUV pulses are measured in the field of the IR lasers. By varying the time delay between the laser and the XUV pulse, their cross-correlation is built either by the laser-induced energy shift<sup>2</sup> or by the laser-broadened spectral width.<sup>3</sup> Based on the quantum mechanical formulation of laser-dressed photoionization,<sup>4,5</sup> photoelectron spectra have been experimentally measured, and pulse duration of a few hundred attoseconds<sup>2</sup> has been determined. Most recently, this technique has also been used to characterize directly the electric field of a few-cycle laser pulse.<sup>6</sup> In the generating and characterizing XUV pulses from these time-resolved measurements, so far only linearly polarized lasers have been used.

An alternative approach to making single attosecond pulses is through high harmonic generation using the polarization gating method.<sup>7-13</sup> Using a laser composed of two opposite circular polarizations, a supercontinuum covering the plateau and the cutoff region of the harmonic spectrum has been recently generated.<sup>14</sup> This method is illustrated in Fig. 1. By superimposing a left-circularly polarized pulse of about 5 fs with a delayed (by about 5 fs) right-circularly polarized pulse, the ellipticity of the combined pulse is almost zero over a short time interval near  $t=0$ .<sup>12</sup> In Fig. 1, it can be seen that within this interval, less than an optical cycle, the electric field of one of the two orthogonal components vanishes, and the electric field is almost linearly polarized. The radiation generated from such a pulse can be calculated and a supercontinuum spectrum is generated. This supercontinuum is expected to correspond to XUV pulses as short as 200 as. However, this duration has not been determined experimentally as yet. In this paper, we discuss a technique that can be used to measure the time-dependent electric field of the attosecond pulses. The method employs the cross correlation between the attosecond pulses with the circularly polarized lasers that were used to generate the attosecond pulse.

In such measurements, the attosecond pulse will be delayed by approximately 5 fs so that the generated photoelectrons only interact with the portion ( $t > 5$  fs) of the laser pulse that is almost circularly polarized. To simplify the analysis, we use an ideal circularly polarized field to represent the laser. By refocusing the XUV pulse and the fundamental circularly polarized laser into the argon gas, the XUV pulse characterization will be determined from the measured angle-resolved photoelectron spectra. Such a setup involves XUV photoionization assisted by a short circularly polarized laser. The basic theory for such cross correlation measurement has been

---

Further author information: (Send correspondence to Z.X.Z.)

Z.X.Z.: E-mail: zzhao@ksu.edu, Telephone: 1 785 532 1635

Z.C.: E-mail: chang@phys.ksu.edu, Telephone: 1 785 532 1621

Ultrafast X-Ray Detectors, High-Speed Imaging, and Applications, edited by Stuart Kleinfelder, Dennis L. Paisley, Zenghu Chang, Jean-Claude Kieffer, Jerome B. Hastings, Proc. of SPIE Vol. 5920 (SPIE, Bellingham, WA, 2005) · 0277-786X/05/\$15 · doi: 10.1117/12.616996

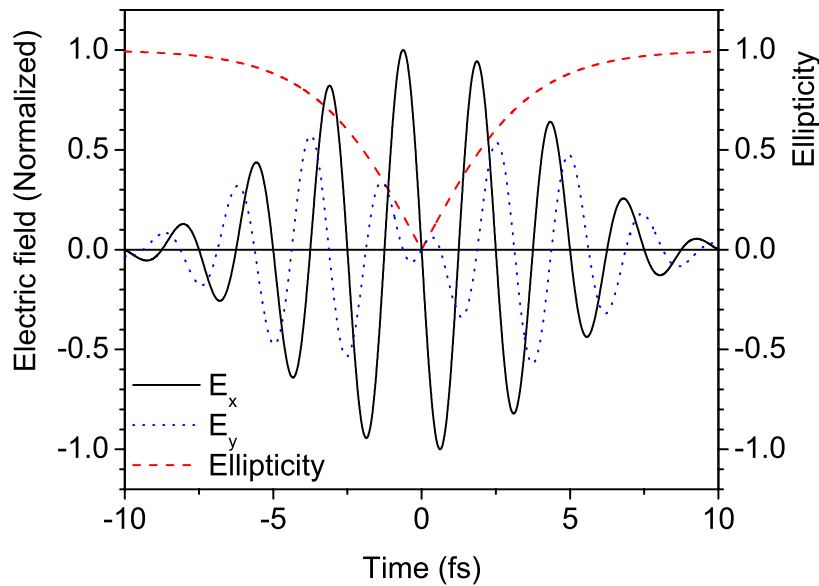


**Figure 1.** The time-dependence of the ellipticity and the two perpendicular electric field components of a laser pulse resulting from combining a left-hand circularly polarized pulse and a right-hand circularly polarized pulse. The pulse duration for both circular pulses is 5 fs and the delay between them is 5 fs. The solid and dotted lines represent the two orthogonal field components and the dashed line shows the ellipticity. Note that the small window of vanishing ellipticity or polarization gating where the combined field is nearly linearly polarized.

addressed by Itatani *et al.*<sup>5</sup> In this paper we examine in detail the laser-assisted photoelectron spectra by taking the angle-dependent photoionization cross section into account. We first studied theoretically the angle-resolved photoelectron spectra for such experiments by changing the attosecond pulse parameters, in particular, the pulse duration and the chirp.<sup>13</sup> We illustrate how the electron spectra change with these parameters. From the calculated electron spectra we then showed how to retrieve the attosecond XUV pulse parameters. This technique is expected to be used to determine the attosecond pulses in the time domain when electron spectra from such cross correlation experiments become available.

In Section 2, we review the theory of laser-assisted photoionization and apply it to the photoionization in the presence of a circularly polarized laser pulse. In section 3, we address the photoionization of Ar atoms by monochromatic light. The atomic structure parameters from these calculations will be used in Section 4 to generate “theoretical” photoionization electron spectra by attosecond pulses in the presence of circularly polarized lasers. We first explore how the electron spectra change with the pulse duration, and then how they change with the chirp. In Section 5 we discuss how to retrieve the attosecond XUV pulse parameters from the given angle-resolved electron spectra. The last Section gives a short conclusion. Atomic units will be used throughout in this paper unless otherwise indicated.

## 2. QUANTUM THEORY OF LASER-ASSISTED PHOTOIONIZATION

Consider an atom in a single-electron approximation under the influence of a laser field. The time-dependent Schrödinger equation (TDSE) in the length gauge is given by

$$i \frac{\partial \Psi(\vec{r}, t)}{\partial t} = \left[ -\frac{1}{2} \nabla^2 + V(\vec{r}) - \vec{r} \cdot \vec{E}(t) \right] \Psi(\vec{r}, t), \quad (1)$$

where  $V(\vec{r})$  is the atomic potential and  $E(t)$  is the external laser field. Dipole approximation is applied for the laser-atom interaction. To solve this equation, the following assumptions (strong field approximation) can be made:

1. No depletion of the ground state;
2. Neglect the influence of Coulomb field on the electrons in the continuum so that they can be treated as free particles moving in the laser field (Volkov state);
3. No other intermediate bound states contribute, i.e., assume that the atom has only one bound state and continua.

The time-dependent wave function can thus be expanded as

$$\Psi(\vec{r}, t) = e^{iI_p t} \left( |0\rangle + \int d\vec{p} b(\vec{p}, t) |\vec{p}\rangle \right), \quad (2)$$

where  $I_p$  is the ionization potential of the ground state  $|0\rangle$ , and  $|\vec{p}\rangle$  denotes the continuum electron with momentum  $\vec{p}$ . The TDSE can be solved semi-analytically in this approximation, and the amplitude of the continuum electron  $|\vec{p}\rangle$  is given by

$$b(\vec{p}, t) = i \int_{-\infty}^t dt_1 \sum_{\vec{p}'} \langle \vec{p} | \vec{p}'(t, t_1) \rangle \langle \vec{p}'(t, t_1) | \vec{r} \cdot \vec{E}(t_1) | 0 \rangle e^{iI_p(t_1-t)} \quad (3)$$

where  $|\vec{p}'(t, t_1)\rangle$  is the Volkov state describing a free particle moving in a laser field and is given by

$$|\vec{p}'(t, t_1)\rangle = \frac{1}{(2\pi)^{3/2}} e^{i(\vec{p} + \vec{A}(t) - \vec{A}(t_1)) \cdot \vec{r}} e^{i \int_{t_1}^t dt'' (\vec{p} + \vec{A}(t) - \vec{A}(t''))^2 / 2}, \quad (4)$$

where  $\vec{A}(t)$  is the vector potential related to the electric field by

$$\vec{E}(t) = -\frac{\partial \vec{A}}{\partial t}. \quad (5)$$

The transition amplitude can be written explicitly as given in<sup>15</sup>:

$$b(\vec{p}, t) = i \int_{-\infty}^t dt_1 \vec{E}(t_1) \cdot \vec{d}[\vec{p} + \vec{A}(t) - \vec{A}(t_1)] \exp \left\{ -i \int_{t_1}^t dt'' \left[ \frac{(\vec{p} + \vec{A}(t) - \vec{A}(t''))^2}{2} + I_p \right] \right\}, \quad (6)$$

where  $\vec{d}(\vec{p})$  is the dipole transition moment from the ground state to the continuum  $|\vec{p}\rangle$ . This equation has been derived in length gauge,<sup>15, 16</sup> in acceleration gauge,<sup>17</sup> and in velocity (radiation) gauge.<sup>18</sup>

This approximation is further applied to the two-color photoionization of atoms by a combination of a linearly polarized XUV pulse and a linearly or circularly polarized laser pulse.<sup>4, 5</sup> In such a setup, the cross correlation of the two pulses is established through the laser-assisted photoionization, which provides a possible way of measuring the duration (a few hundred attoseconds) of the short XUV pulse. The photoelectron spectrum is given by Eq. (6) at  $t$  goes to  $\infty$  (the vector potential vanishes in our choice):

$$b(\vec{p}) = i \int_{-\infty}^{\infty} dt' \vec{E}(t') \cdot \vec{d}[\vec{p} - \vec{A}(t')] \times \exp \left\{ -i \int_{t'}^{\infty} \frac{[\vec{p} - \vec{A}(t'')]^2}{2} dt'' + iI_p t' \right\}. \quad (7)$$

By considering the different photon energy scales of the XUV and the laser field, this equation can be further simplified. For a weak laser field, ionizations by the laser field itself can only go through a multiphoton process.

In the non-resonant case, multiphoton ionizations are much weaker than ionizations by single photon. Thus in the process of generating the continuum, we can neglect the contribution of the laser field. This assumption can be checked numerically by calculating the ionization probability by the laser field and by the XUV pulse individually. In propagating of the free electron in the field, we neglect the XUV pulse, since the vector potential is inversely proportional to the photon energy.

Now let us consider the photoionization of Ar atoms by XUV pulses assisted by a circularly polarized laser field. Electrons that are born at different times within the XUV pulse gain additional time-dependent drift velocity from the laser field, which is rotating in time. The XUV pulse with duration  $\tau_x$  and photon energy  $\omega_x$  can be generally described by

$$\vec{E}_x(t) = \text{Re}\{E_{0x}e^{-\sigma(1-i\xi)t^2}e^{i\omega_x t}\vec{e}_x\}, \quad (8)$$

where  $\sigma = 2 \ln 2/\tau_x^2$ , and  $\xi$  is a dimensionless chirp parameter. The XUV pulse is linearly polarized along x direction with intensity  $10^{12}$  W/cm<sup>2</sup> and mean photon energy 35 eV. A circularly polarized laser field is characterized by an electric field

$$\vec{E}_l(t) = \frac{1}{\sqrt{2}}E_0(t)[\cos(\omega_l t + \phi)\vec{e}_x + \sin(\omega_l t + \phi)\vec{e}_y] \quad (9)$$

that has a Gaussian shape with FWHM of 5 fs, intensity of  $5 \times 10^{13}$  W/cm<sup>2</sup>. The central wavelength of the laser is taken to be 750 nm.

For electrons born at time  $t$ , they gain a drift momentum (proportional to the vector potential of the laser field) given by

$$\vec{A}_l(t) = - \int_{-\infty}^t \vec{E}_l(t) dt. \quad (10)$$

For the convenience of analysis, if the envelope is slow varying, the drift velocity can be approximated by

$$\vec{A}_l(t) \cong \frac{1}{\sqrt{2}\omega_l}E_0(t)[- \sin(\omega_l t + \phi)\vec{e}_x + \cos(\omega_l t + \phi)\vec{e}_y]. \quad (11)$$

According to the strong-field approximation,<sup>15,16</sup> the laser-assisted photoelectron spectrum is again given by Eq. (7). From the saddle point analysis, most of the contribution to the time integral comes from the time  $t_s$  satisfying the stationary phase condition

$$\frac{1}{2}[\vec{p} - \vec{A}_l(t_s)]^2 = E_0, \quad (12)$$

which gives the classical model.<sup>2,3</sup> It represents energy conservation for photoionization in the presence of lasers, where,  $E_0 = \omega_x - I_p$ . In the calculation, integration over time in Eq. (7) is performed numerically. If the electron is born with momentum  $\vec{p}_0$  ( $p_0 = \sqrt{2E_0}$ ) at  $t_s$ , the final momentum will be given by  $\vec{p} = \vec{p}_0 + \vec{A}_l(t_s)$ . Electrons born at different times will gain momentums along different angles. The angular width is directly related to the pulse duration, thus providing the possibility of measuring the attosecond pulses from the angle-resolved spectra as illustrated in Fig. 2. In the reality, the final angular distribution is convoluted to the distribution of  $\vec{p}_0$ .

### 3. CROSS SECTIONS AND ASYMMETRY PARAMETERS FOR PHOTOIONIZATION OF AR

In the theory discussed above, the XUV radiation induced transition dipole moment is required to be known. In the single active electron model,<sup>19</sup> the argon atom is described by a model potential

$$V(r) = -(1 + 5.4e^{-r} + 11.6e^{-3.682r})/r. \quad (13)$$

Starting from the occupied 3p orbital, the electron is released to s-wave or d-wave continuum through one-photon photoabsorption. The radial dipole matrix elements to  $\epsilon_s$  ( $R_-$ ) and  $\epsilon_d$  ( $R_+$ ) continuum states are given by

$$R_{-(+)} = \int_0^\infty r P_{3p} P_{\epsilon_s(\epsilon_d)} dr, \quad (14)$$

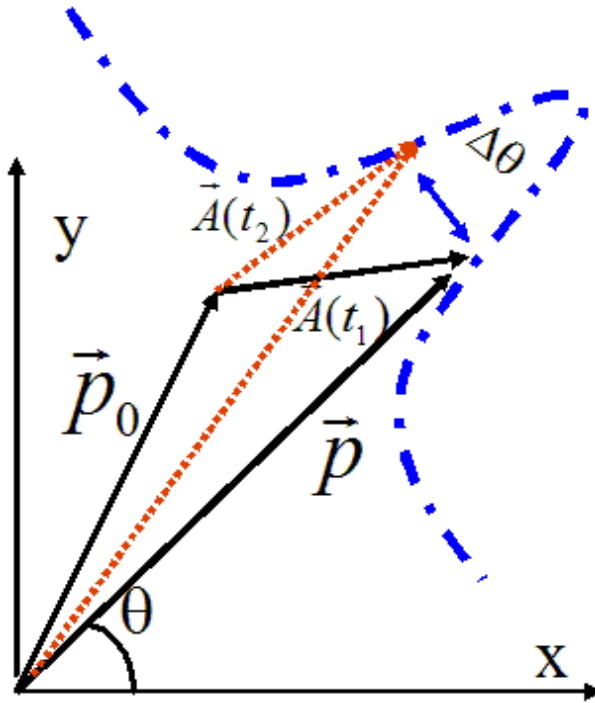


**Figure 2.** Illustration of the final momentum distribution of electrons born in a circularly polarized laser field. An electron born at the beginning of the pulse,  $t_1$ , gains a drift momentum  $\vec{A}(t_1)$ , and thus has the final momentum  $\vec{p}$  with angle  $\theta$ . At the ending of the pulse, time  $t_2$ , the electron has different final momentum. The angular width is thus related to the pulse duration directly.

where the P's are the r-weighted radial wavefunctions. Since there are six 3p valence electrons in the ground state of argon, the total cross section  $\sigma_{tot}$  is proportional to

$$|d|^2 = 6\left(\frac{1}{3}R_-^2 + \frac{2}{3}R_+^2\right) \quad (15)$$

where  $d$  is the magnitude of the total transition dipole moment.

The angular distribution of the photoelectrons by a linearly polarized light is given by

$$\frac{d\sigma}{d\Omega} = \frac{\sigma_{tot}}{4\pi} \left[1 + \beta \frac{3\cos^2\theta - 1}{2}\right], \quad (16)$$

where  $\theta$  is the angle of the electron's final momentum with respect to the light polarization direction, and  $\beta$  is the asymmetry parameter that can be calculated using the method described in.<sup>20</sup> Knowing the  $\beta$  parameter and the total transition dipole moment, in the same spirit of obtaining the differential cross section, we can define an effective angular dependent transition dipole moment for later calculating laser-assisted photoionization.

Figure 3 shows the calculated (a)  $|d|^2$  and (b) the  $\beta$  parameter, versus the photon energy of the monochromatic XUV light. The results from this simple calculation show reasonably good agreement with the more elaborate many-electron calculations,<sup>21,22</sup> including the position of the Cooper minimum. A direct numerical solution of the time-dependent Schrödinger equation for the ionization of argon atom in a short XUV pulse has also been carried out with these pulse parameters: mean photon energy, 35 eV; pulse duration, 100 as; peak intensity,  $10^{12}$  W/cm<sup>2</sup>. The photoelectron spectrum from such a calculation is presented in Fig. 3(c). Since the interaction is in the perturbation regime, the spectral intensity distribution of the XUV pulse can be obtained by dividing the electron spectral density by the photoionization cross section, as shown in dashed lines in Fig. 3(c). Assuming that the pulse is transform-limited, the XUV pulse in the time-domain can be obtained directly by a simple Fourier transformation. However, such an assumption is not generally valid.

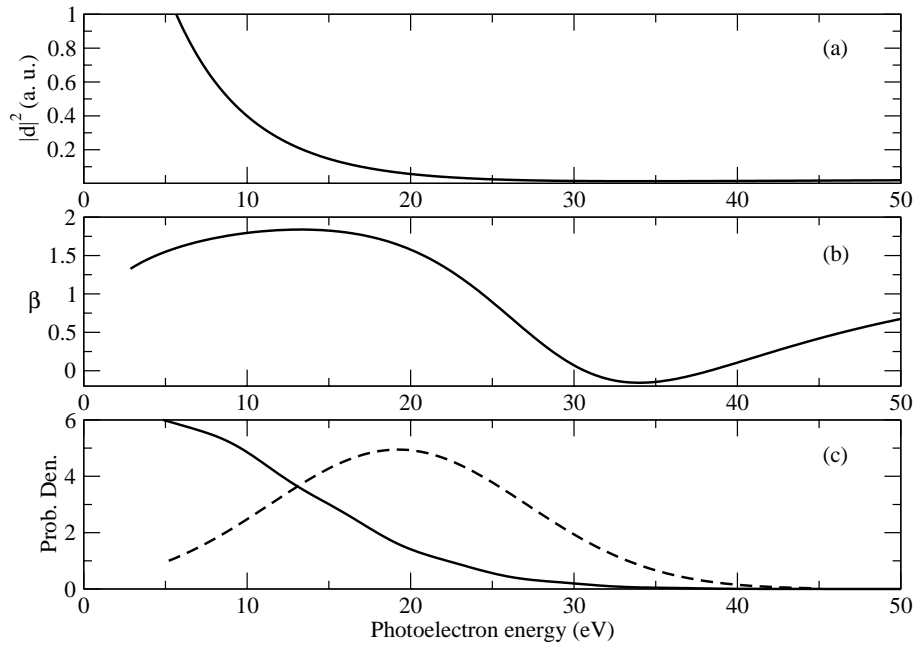
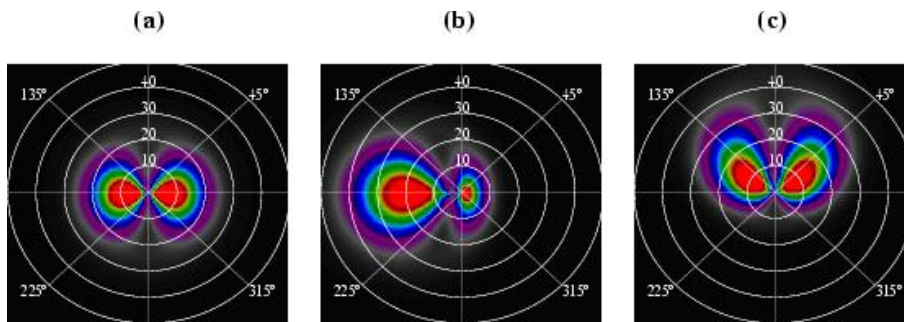


**Figure 3.** (a) The square of the dipole transition moment and (b) the asymmetry parameter  $\beta$  from the ground state of Ar by monochromatic light. (c) The ionization probability density vs photoelectron energy of Ar ionized by an XUV pulse which has mean photon energy of 35 eV, duration of 0.1 fs and peak intensity of  $10^{12}$  W/cm<sup>2</sup>. Dashed lines represent the spectral shape of the XUV pulse.

#### 4. ANGLE-RESOLVED PHOTOELECTRON ENERGY SPECTRA

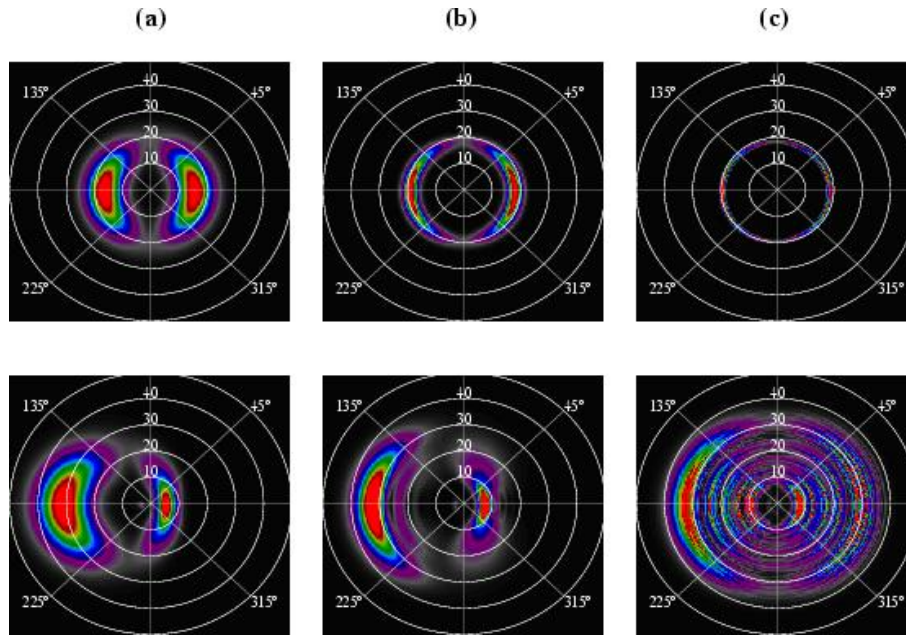
##### 4.1. Transform-limited XUV pulses

First we consider transform-limited XUV pulses for which the chirp parameter is zero. XUV pulse parameters are chosen as that used in Fig. 3. Note that the XUV photon energy of 35 eV corresponds to the 21th-order high harmonics from the Ti:Sapphire laser field with a wavelength 750 nm. Laser intensity was chosen to be  $5 \times 10^{13}$  W/cm<sup>2</sup> so that the ionization probability by the XUV itself (intensity is  $10^{12}$  W/cm<sup>2</sup>) is two orders higher than the ionization probability by the laser field. The two pulses peak at the same time  $t = 0$ . The polarization direction of the XUV pulse is defined as the x-axis (zero angle). The drift velocity at  $t = 0$  is along y direction if the laser phase is zero and -x direction if laser phase is  $\pi/2$ .



**Figure 4.** (a) Energy and angular distributions of photoelectrons from Ar by a single XUV pulse of duration (FWHM) 100 as. The polarization of the XUV pulse is along the x-axis from which the angles of the photoelectrons are measured. (b) and (c), electron spectra by XUV pulses assisted by a circularly polarized laser with phase of  $\pi/2$  and 0, respectively. The XUV pulse was assumed to be not chirped.

For XUV photon energy of 35 eV, the asymmetry parameter  $\beta$  is about 1.5, thus the laser-free photoelectrons peak at 0 and 180 degrees as shown in Fig. 4(a). Due to the stronger signal along the XUV polarization direction (x-axis), smaller detection angle is required when the detector is along the x-axis. When a laser field is present, the spectrum is deformed. Fig. 4(b) and Fig. 4(c) show the laser-assisted photoelectron spectra for laser phase of  $\pi/2$  and 0, respectively. When the drift velocity is along the  $-x$  direction ( $\phi = \pi/2$ , Fig. 4(b)), more electrons are found in the  $-x$  direction and the energy distribution is stretched in the same direction which makes the detection more efficient than the case of laser phase of 0 (Fig. 4(c)). Clearly, a phase-stabilized laser of phase  $\phi = \pi/2$  is more desirable. In the following, we will only consider the laser phase of  $\phi = \pi/2$  unless otherwise indicated



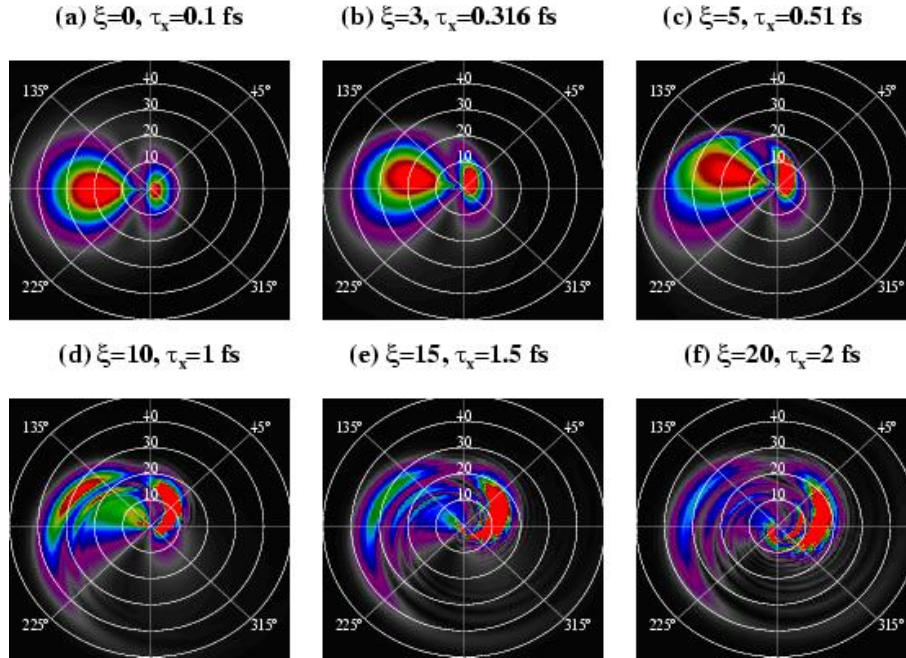
**Figure 5.** Dependence of photoelectron spectra on the XUV pulse durations. The upper row is for laser-free photoionization and the lower row is for laser-assisted photoionization where the laser phase was chosen to be  $\pi/2$ . From (a) to (c) the XUV pulse durations are 0.2, 0.5 and 2 fs, respectively. The XUV pulses are assumed to have no chirp.

Figure 5 shows how the electron spectra change with increasing XUV pulse duration. As XUV duration increases, the energy width of laser-free photoelectron spectra decreases. On the other hand, when a circularly polarized laser is present, the distribution of the drift velocity that the electrons gain during the XUV pulse duration becomes broader in the angle; thus the resulting photoelectron spectra show broader angular width. When the XUV pulse duration approaches the laser period (Fig. 5(c)), ring-like sideband structures appear following the trajectory of laser's vector potential. The ring-like structures were also observed for linearly polarized laser-assisted photoionization by a train of attosecond pulses.<sup>23</sup>

In short, if the XUV pulses are transform-limited, we have:

1. The electron energy width for a given angle decreases as the XUV pulse duration increases.
2. The electron angular width for a given energy becomes broader as XUV pulse duration increases.
3. The electron's momentum image extends in all directions and sideband structure begins to emerge as the XUV pulse duration approaches laser's optical period.

Based on the pulse duration dependence of the spectra, the duration of the attosecond pulse might be deduced by mapping the measured electron velocity image in accordance with the principle of frequency resolved optical gating (FROG).<sup>24</sup> As suggested by Itatani *et al.*,<sup>5</sup> the pulse duration can be retrieved from the angular distribution of electron momentum at a given energy. We will discuss this further.



**Figure 6.** Photoelectron spectra by laser-assisted XUV pulses with different chirp parameters and pulse durations as indicated in the figure. The frequency width of XUV pulse is fixed as 18.25 eV.

## 4.2. Chirp-dependence

In the previous section, we discussed how the electron spectra change with the duration of the XUV pulses when they are transform-limited. However, for transform-limited XUV pulses, the pulse duration can be obtained directly from the bandwidth of the photoelectron energy spectrum at any angle, without applying the laser field, as discussed earlier. In general, the chirp parameter of the XUV pulse has to be determined in order to obtain the pulse duration.

For the XUV pulse described in Eq. (8), with nonzero chirp parameter, the frequency bandwidth is given by

$$\Delta\omega = \frac{4 \ln 2}{\tau_x} \sqrt{1 + \xi^2}. \quad (17)$$

We will examine laser-assisted electron spectra with fixed frequency bandwidth by varying the pulse duration and the chirp  $\xi$  simultaneously. In Fig. 6, we present six cases of chirp parameters and pulse durations: (a)  $\xi=0$ ,  $\tau_x=0.1$  fs; (b)  $\xi=3$ ,  $\tau_x=0.32$  fs; (c)  $\xi=5$ ,  $\tau_x=0.51$  fs; (d)  $\xi=10$ ,  $\tau_x=1$  fs; (e)  $\xi=15$ ,  $\tau_x=1.51$  fs and (d)  $\xi=20$ ,  $\tau_x=2$  fs.

With the XUV pulse frequency bandwidth fixed, the laser-free photoionization spectra are the same for all the six cases (see Fig. 6(a)). Thus, the pulse duration can not be resolved by XUV photoionization alone. As the chirp increases from (b) to (f), the spectral image twists and splashes toward the left (we used left-circularly polarized laser). This behavior can be understood from the modified stationary phase equation (Eq. (12)):

$$\frac{1}{2}[\vec{p} - \vec{A}_l(t)]^2 = E_0 - 2\sigma\xi t = \Omega(t). \quad (18)$$

In contrast to the zero-chirp case, the electron is born with a time-dependent instantaneous energy in a chirped pulse. Thus the final electron momentum is not just rotated by the laser field but also stretched in magnitude due to the chirp. In this case, we can not determine the pulse duration from the angular distribution of the electron momentum at a given energy. Instead, at each angle we can define the center of gravity energy  $E(\theta)$  (see Fig. 7). By focusing on this trace for angles larger than  $180^\circ$ , we note that  $E(\theta)$  increases monotonically



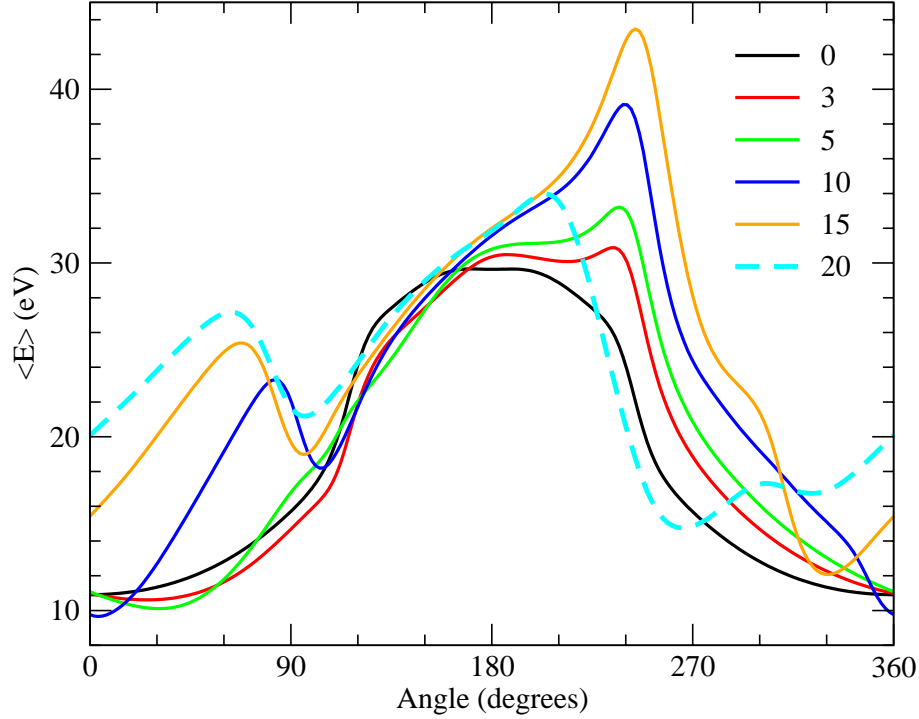


**Figure 7.** The center of gravity energy of the photoelectrons vs the electron's angle for different chirp parameters from 0 to 20 of the XUV pulses. The width of the XUV pulse is fixed at 18.25 eV. Note the shift to the higher energy as the chirp parameter increases until at the highest chirp where the pulse duration is close to the optical period.

with increasing chirp, until for the large chirp parameter of 20 where the duration of the XUV pulse of 2.0 fs is close to the laser period. This trace, combining with the angular width, qualitatively illustrates the chirp and pulse duration dependence on the XUV pulses in the time-domain.

### 4.3. Double XUV pulses

Next we consider a pulse train consisting of double pulses without chirp, separated by  $T_0/2$  (i.e., one half of the laser period),

$$E_x(t - T_0/4) + E_x(t + T_0/4). \quad (19)$$

Each pulse has a duration of 0.2 fs and a corresponding peak intensity  $10^{12}$  W/cm<sup>2</sup>. When the polarization gating is not short enough, such a train of two attosecond pulses is generated.

For such a pulse train, the laser-free photoelectron energy spectra consist of two rings separated by  $2\omega_l$ , see Fig. 8(a). When the laser field is present, the spectra are distorted but have two identical pairs. In Fig. 8, the laser phases are  $0, \pi/4, \pi/2$ , respectively, from (b) to (d). In (b) electrons generated by the left pulse experience a  $+x$  shift, while electrons generated by the right pulse experience a  $-x$  shift. Thus the total electron spectra are stretched along the  $x$ -axis. In (c), electrons generated by the two pulses shift about half way toward the 45 degrees (and 225 degrees) line. In (d), the shifting to this diagonal line is complete and the electron spectrum shows a butterfly shape.

## 5. RETRIEVING THE XUV PULSE INFORMATION

The laser-free photoionization spectrum is obtained from this equation

$$b(\vec{p}) = i \int_{-\infty}^{\infty} dt \vec{d}(\vec{p}) \cdot \vec{E}_x(t) \exp[i(1/2)p^2 t + iI_p t]. \quad (20)$$

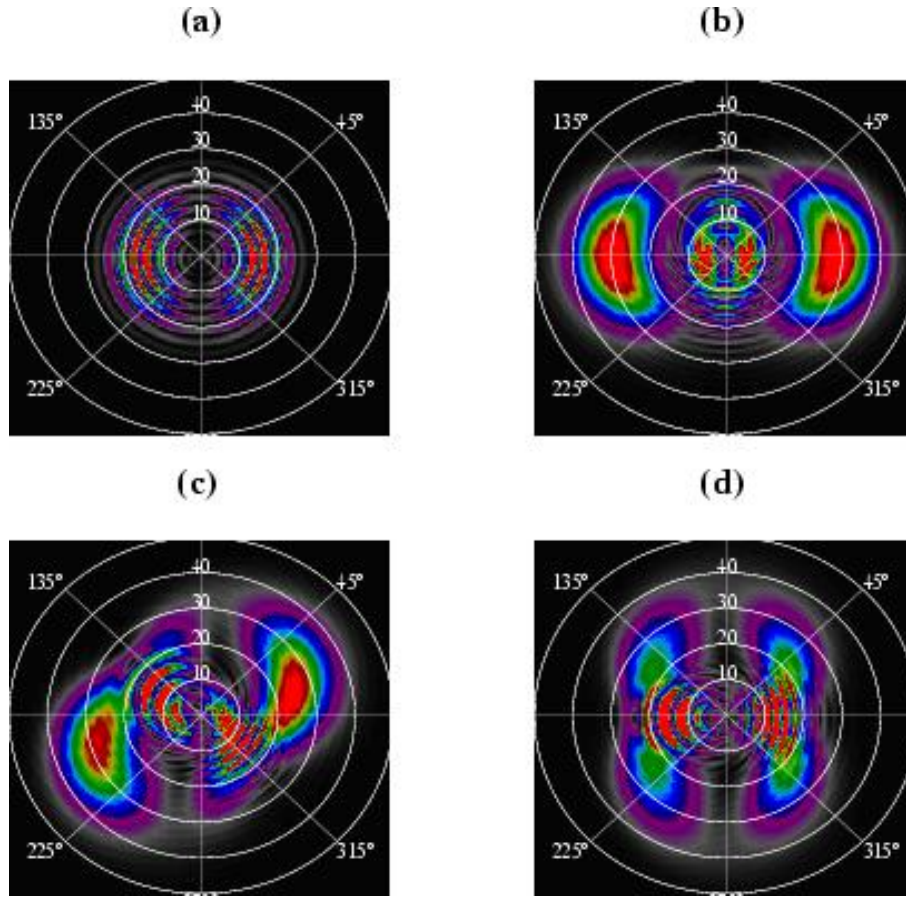


**Figure 8.** Photoelectron spectra by a train of two attosecond XUV pulses: (a) no laser ; (b),(c),(d), with lasers, of phase 0,  $\pi/4$  and  $\pi/2$ , respectively.

If both the magnitude and phase of the photoelectron spectrum are known, the pulse information can be retrieved directly by inverse Fourier transformation. However, only  $|b(\vec{p})|^2$  is available experimentally. In order to obtain the phase information, one must rely on the additional information supplied by the laser-assisted photoionization measurement which builds the cross-correlation between the XUV pulse and the laser pulse. Our procedure of retrieving the XUV pulse can be described as follows: 1) using the measured laser-free spectra as input; 2) starting with a simple guess of the phase of  $b(\vec{p})$  to reconstruct the XUV pulse; 3) use the guessed XUV pulse to calculate laser-assisted photoelectron spectra; 4) compare the calculated spectra with the measured spectra with the discrepancy recorded as the error function; 5) repeat processes 2) to 4) with another guess until the best fitting is found.

This fitting process can be improved by using genetic algorithm. In the simplest case, if we assume the XUV pulse has a Gaussian profile and is linearly chirped, then only one parameter must be fitted based on Eq. (17). For the general pulse shape and chirp, we can either discretize the phase into  $N$  slices and vary them independently to find the best fit, or expand the phase into a polynomial

$$\phi(\omega) = \sum_{i=1}^N c_i (\omega - \omega_0)^i \quad (21)$$

where  $\omega_0$  is the center frequency, and the second order term corresponds to the linear chirp of the pulse. Our simulation shows that the latter method converges faster and is indeed used to retrieve the pulse information in the following example.

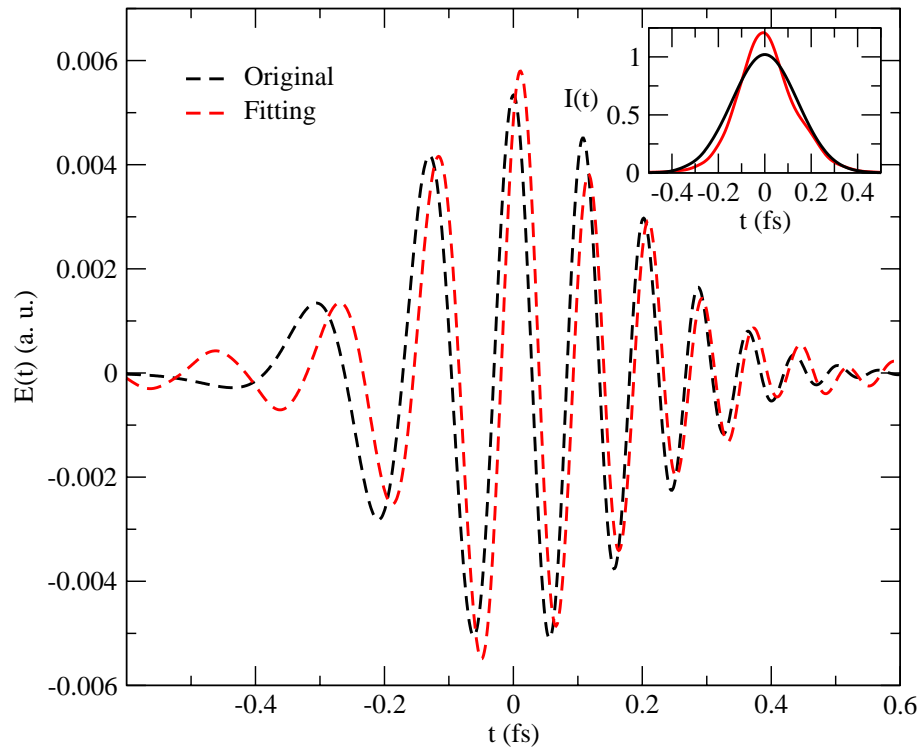


**Figure 9.** Comparison of the retrieved electric field with the original field. The inset shows the intensity profile of the original and the retrieved pulses, in units of  $10^{12} \text{W/cm}^2$ .

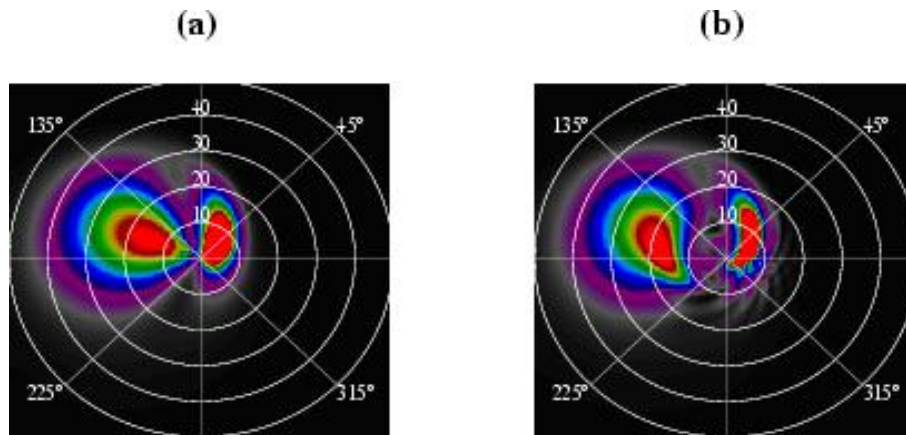


**Figure 10.** Comparison of the photoelectron spectra calculated using (a) the original pulse and (b) the retrieved pulse, at a different time delay of  $-0.2 \text{ fs}$ .

To illustrate the retrieval method, we assume the measured photoelectron spectrum as given as in Fig. 6(b). We used the procedure described above to retrieve the XUV pulse information. In the simulation, we chose  $N=5$ . The retrieved pulse is compared to the original pulse in Fig. 9. Good agreement can be seen in both the magnitude and the phase of the retrieved electric field. The agreement in the intensity profile is shown in the inset. As a further check on how well the retrieved pulse agrees with the original one, we also simulate the electron spectrum at time delay of -0.2 fs using both the original and the retrieved pulses where the first spectrum was supposedly determined experimentally. As shown in Fig. 10, the two spectra are in reasonable good agreement with each other. In the retrieving process, we assume the carrier-envelope phase (90 degrees) and the profile of the laser pulse is known. If the phase has uncertainty, e.g., 80 degrees instead of 90 degrees, we obtain roughly the same pulse duration.

## 6. SUMMARY AND CONCLUSION

In summary, we performed calculations of angle-resolved photoelectron spectra of Ar atoms in the combined field of an attosecond XUV pulse and a circularly polarized laser pulse. We examined first theoretically how the electron spectra, including the angular distributions, depend on the pulse duration and the chirp parameter of the XUV light pulse. We also showed how to retrieve or measure the pulse duration and the chirp parameter of such an attosecond XUV pulse if the angle-resolved electron spectra were available from experiments. The method requires that the few-cycle lasers be well characterized already, including its carrier envelope phase.

By focusing on the main features of the laser-assisted photoelectron spectra such as the mean kinetic energy of the photoelectron at a given angle, we showed that it is possible to retrieve the pulse duration and the chirp parameter from the measured electron energy and angular distributions at a given time delay. Systematic check can be further made through multiple measurements by varying the time delay between the XUV and IR pulses. For attosecond XUV pulses generated by the polarization gating method, the procedure presented in this paper is expected to be used to characterize the pulse when photoelectron spectra from such cross-correlation measurements become available.

## ACKNOWLEDGMENTS

This work is in part supported by Chemical Sciences, Geosciences and Biosciences Division, Office of Basic Energy Sciences, Office of Science, U.S. Department of Energy.

## REFERENCES

1. T. Brabec and F. Krausz, "Intense few-cycle laser fields: Frontiers of nonlinear optics," *Rev. Mod. Phys.* **72**, p. 545, 2000.
2. M. Drescher, M. Hentschel, R. Kienberger, G. Tempea, C. Spielmann, G. A. Reider, P. B. Corkum, and F. Krausz, "X-ray pulses approaching the attosecond frontier," *Science* **291**, p. 1923, 2001.
3. M. Hentschel, R. Kienberger, C. Spielmann, G. A. Reider, N. Milosevic, T. Brabec, P. Corkum, U. Heinzmann, M. Drescher, and F. Krausz, "Attosecond metrology," *Nature (London)* **414**, p. 509, 2001.
4. M. Kitzler, N. Milosevic, A. Scrinzi, F. Krausz, and T. Brabec, "Quantum theory of attosecond xuv pulse measurement by laser dressed photoionization," *Phys. Rev. Lett.* **88**, p. 173904, 2002.
5. J. Itatani, F. Quéré, G. L. Yudin, M. Y. Ivanov, F. Krausz, and P. B. Corkum, "Attosecond streak camera," *Phys. Rev. Lett.* **88**, p. 173903, 2002.
6. E. Goulielmakis, M. Uiberacker, R. Kienberger, A. Baltuska, V. Yakovlev, A. Scrinzi, T. Westerwalbesloh, U. Kleineberg, U. Heinzmann, M. Drescher, and F. Krausz, "Direct measurement of light waves," *Science* **305**, p. 1267, 2004.
7. P. B. Corkum, N. H. Burnett, and M. Y. Ivanov, "Subfemtosecond pulses," *Opt. Lett.* **19**, p. 1870, 1994.
8. M. Ivanov, P. B. Corkum, T. Zuo, and A. Bandrauk, "Routes to control of intense-field atomic polarizability," *Phys. Rev. Lett.* **74**, p. 2933, 1995.
9. P. Antonie, B. Piraux, D. B. Milosevic, and M. Gajda, "Generation of ultrashort pulses of harmonics," *Phys. Rev. A* **54**, p. R1761, 1996.

10. V. T. Platonenko and V. V. Strelkov, "Single attosecond soft-x-ray pulse generated with a limited laser beam," *J. Opt. Soc. Am. B* **16**, p. 435, 1999.
11. V. Strelkov, A. Zair, O. Tcherbakoff, R. López-Martens, E. Cormier, E. Mével, and E. Constant, "Generation of attosecond pulses with ellipticity-modulated fundamental," *Appl. Phys. B* **78**, p. 879, 2004.
12. Z. Chang, "Single attosecond pulse and xuv supercontinuum in the high-order harmonic plateau," *Phys. Rev. A* **70**, p. 043802, 2004.
13. Z. Chang, "Chirp of the single attosecond pulse generated by a polarization gating," *Phys. Rev. A* **71**, p. 023813, 2005.
14. B. Shan, S. Ghimire, and Z. Chang, "Generation of attosecond extreme ultraviolet supercontinuum by a polarization gating," *J. Modern. Optics* **52**, p. 277, 2004.
15. M. Lewenstein, P. Balcou, M. Y. Ivanov, Anne L'Huillier, and P. B. Corkum, "Theory of high-harmonic generation by low frequency laser fields," *Phys. Rev. A* **49**, p. 2117, 1994.
16. L. V. Keldysh, "Ionization in the field of a strong electromagnetic wave," *Sov. Phys. JETP* **20**, p. 1307, 1965.
17. F. H. Faisal, "Multiple absorption of laser photons by atoms," *J. Phys. B* **6**, p. L689, 1973.
18. H. R. Reiss, "Effect of an intense electromagnetic field on a weakly bound system," *Phys. Rev. A* **22**, p. 1786, 1980.
19. E. S. Toma and H. G. Muller, "Calculation of matrix elements for mixed extreme-ultraviolet-infrared two-photon above-threshold ionization of argon," *J. Phys. B* **35**, p. 3435, 2002.
20. D. J. Kennedy and S. T. Manson, "Photoionization of the noble gases: Cross sections and angular distributions," *Phys. Rev. A* **5**, p. 227, 1972.
21. F. A. Parpia, W. R. Johnson, and V. Radojevic, "Application of the relativistic local-density approximation to photoionization of the outer shells of neon, argon, krypton and xenon," *Phys. Rev. A* **29**, p. 3173, 1984.
22. M. Y. Adam, P. Morin, and G. Wendin, "Photoelectron satellite spectrum in the region of 3s Cooper minimum of argon," *Phys. Rev. A* **31**, p. 1426, 1985.
23. S. A. Aseyev, Y. Ni, L. J. Frasinski, H. G. Muller, and M. J. J. Vrakking, "Attosecond angle-resolved photoelectron spectroscopy," *Phys. Rev. Lett.* **91**, p. 223902, 2003.
24. R. Trebino, K. W. DeLong, D. N. Fittinghoff, J. N. Sweetser, M. A. Krumbügel, and B. A. Richman, "Measuring ultrashort laser pulses in the time-frequency domain using frequency-resolved optical gating," *Rev. Sci. Instrum.* **68**, p. 3277, 1997.